Received: 13 May 2020 | Revised: 16 August 2020 | Accepted: 20 August 2020

DOI: 10.1111/cas.14634

ORIGINAL ARTICLE

Cancer Science WILEY

A ceRNA network and a potential regulatory axis in gastric cancer with different degrees of immune cell infiltration

Kai Zhang[1,2,3] | Lei Zhang[4] | Yang Mi[1,2] | YouCai Tang[1,2] | FeiFei Ren[1,2] | Bin Liu[1,2] | Yi Zhang[3] | PengYuan Zheng[1,2]

[1]Henan Key Laboratory for Helicobacter pylori & Microbiota and GI Cancer, Marshall Medical Research Center, The Fifth Affiliated Hospital of Zhengzhou University, Zhengzhou, China

[2]Department of Gastroenterology, The Fifth Affiliated Hospital of Zhengzhou University, Zhengzhou, China

[3]Biotherapy Center, The First Affiliated Hospital of Zhengzhou University, Zhengzhou, China

[4]Department of Pediatric Surgery, The First Affiliated Hospital of Zhengzhou University, Zhengzhou, China

Correspondence

PengYuan Zheng and Yi Zhang, Department of Gastroenterology, The Fifth Affiliated Hospital of Zhengzhou University, Zhengzhou, Henan 450052, China.
Emails: medp7123@126.com; yizhang@zzu.edu.cn

Funding information

Excellent Foreign Scientist Studio of Henan Province in China, Grant/Award Number: GZS2018001; Medical science and technology project of Henan Province in China, Grant/Award Number: 2018020224; National Natural Science Foundation of China, Grant/Award Number: 31471330; Zhengzhou Major Collaborative Innovation Project, Grant/Award Number: 18XTZX12003; Medical Service Capacity Improvement project of Henan Province in China, Grant/Award Number: [2017] No. 66

Abstract

Immune cell infiltration is an important indicator of whether tumor patients will benefit from immunotherapy. Gastric cancer is one of the most common tumors in the world, and new indicators of immunotherapy are urgently needed. The aim of this study was to construct ceRNA networks in gastric cancer with different degrees of immune cell infiltration. We analyzed the expression profiles of different gastric cancer with different degrees of immune cell infiltration retrieved from The Cancer Genome Atlas (TCGA) database and found differentially expressed lncRNAs, mRNAs, and miRNAs. A ceRNA regulatory network of gastric cancer with different degrees of immune cell infiltration was constructed using functional annotation, RNA-RNA interaction prediction, correlation analysis, survival analysis, and other comprehensive bioinformatics methods. The interaction and correlation between ceRNAs were verified using experiments on tumor tissues and cell lines. Cell line experiments showed a potential RP11-1094M14.8/miR-1269a/CXCL9 axis that was consistent with the ceRNA theory. qRT-PCR results showed that RP11-1094M14.8 knockdown significantly reduced the expression of CXCL9, and RP11-1094M14.8 overexpression had the opposite effect. The results of clinical analysis of gastric cancer samples showed that RP11-1094M14.8 and CXCL9 were highly expressed in hot tumors, and CXCL9 was positively correlated with a better prognosis for patients. The constructed novel ceRNA network and the potential regulatory axis may provide a comprehensive understanding of the potential mechanisms of development in gastric cancer with different degrees of immune cell infiltration. The RP11-1094M14.8/miR-1269a/CXCL9 axis may serve as a potential immune-therapeutic target for gastric cancer with different degrees of immune cell infiltration.

KEYWORDS

ceRNA, CXCL9, gastric cancer, immune infiltration

Abbreviations: ceRNA, competing endogenous RNA; CTLs, cytotoxic T lymphocytes; DERNAs, differentially expressed RNAs; GC, gastric cancer; IR, immune response; lncRNAs, long non-coding RNAs; miRNA, microRNA; mRNA, messenger RNA; NK, natural killer cells; PPI, Protein-Protein Interaction network; qRT-PCR, quantitative real-time PCR; TCGA, The Cancer Genome Atlas; TME, tumor microenvironment.

Yi Zhang and PengYuan Zheng contributed equally in this study.

1 | INTRODUCTION

Gastric cancer is the fourth most common cancer and the second leading cause of tumor-related death worldwide.[1] Locally advanced GC has a high recurrence rate of approximately 40%-80%.[2] Although significant progress had been achieved in the detection, prevention, diagnosis, and therapeutic strategy in recent years,[3,4] such as the detection of *Helicobacter pylori* infection and immunotherapy, many questions remain unsolved, and GC patients with advanced stages generally experience an extremely poor prognosis.[5] With deepened understanding of the molecular biological characteristics of gastric cancer, new gastric cancer treatment strategies have been examined,[6] and monoclonal antibody-targeted drug therapy and immunotherapy has brought hope to patients with gastric cancer.[7] Tumor immunotherapy is a new kind therapy that uses immunological principles and methods to activate a patient's own immune system and enhance the patient's anti-tumor immune response, which inhibits tumor growth.[8,9]

A diagnostic indicator is important in the prediction of tumor immunotherapy efficiency, which predicts whether patients may benefit from treatment and provides ways in which to choose a more suitable treatment for patients.[10,11] For example, PD-1 is an effective target for tumor immunotherapy, however fewer than 20% of patients benefit from this therapy, and the immune mechanisms involved in the response to these therapeutic interventions remain poorly elucidated, especially in non–small-cell lung cancers and esophagus-gastric cancers.[12,13] The infiltration of immune cells in tumor sites is the basis for effective immunotherapy. Therefore, finding indicators to evaluate immune infiltration and the examination of their potential mechanisms will aid research progress in immunotherapy.

The multifaceted role of lncRNAs in the development of GC had been extensively studied.[14] Competitive endogenous RNA (ceRNA) regulatory networks are significant mechanisms by which lncRNAs may exert huge influences on cancer. In the ceRNA networks,[15-17] lncRNAs act as endogenous molecular sponges that competitively bind to miRNAs,[18] which indirectly regulate the expression level of messenger RNA (mRNA). Numerous experiments have demonstrated that this miRNA-regulated lncRNA and mRNA network is involved in the development, progression, and invasion of cancer.[19] Yvonne et al[20] showed that the tumor suppressor PTEN competed with several ceRNAs in diverse cancers.

Immunotherapy is an important treatment method for tumors, and has shown great clinical value. However, only a subset of patients respond to immunotherapy. The degree of T-cell infiltration is regulated via tumor cell-intrinsic signaling pathways and gene regulatory networks.[21] The role of this regulatory mechanism is not clear in GC. The present study divided the large data of GC patients from the TCGA database into 2 groups based on the different infiltration pattern of T cells in tumors and investigated the regulatory mechanism of different degrees of T-cell infiltration in the immune infiltration gastric cancer.

2 | MATERIALS AND METHODS

2.1 | TCGA data retrieval

The miRNA, mRNA and lncRNA data for gastric cancer patients (RNAseqv2 and miRNA-seq) were downloaded from TCGA database and were sorted into standardized original data for subsequent analysis. Based on the median expression levels of *CD3*, *CD8*, *IFN-γ*, and *GZMB*, patients were defined as high expression or low expression of these 4 genes. We analyzed differentially expressed genes between the hot tumor group (111 patients with $CD3^+CD8^+IFN\text{-}\gamma^+GZMB^+$) and the cold tumor group (116 patients with $CD3^-CD8^-IFN\text{-}\gamma^-GZMB^-$).

2.2 | Identification of differentially expressed lncRNAs, mRNAs, and miRNAs

Differentially expressed mRNA, lncRNA, and miRNA were obtained via screening and analyses of cold and hot tumors. The difference screening parameters were set as $P < .05$ and false discovery rate (FDR) < 0.05 and FC > 1.5. The numbers of differentially expressed mRNAs, lncRNAs and miRNAs were 1082, 97, and 46, respectively.

2.3 | Functional annotation

To illustrate the functional annotations implicated with the DEmRNAs, gene ontology (GO) annotation analysis and Kyoto Encyclopedia of Genes and Genomes (KEGG) pathway enrichment analysis were performed using the "clusterProfiler" package in R software. The significance level (*P*-value) and false-positive rate (FDR) of each signal pathway were calculated using Fisher exact test and multiple comparison test. Therefore, the significant signaling pathway represented by the mRNAs was screened.[22]

2.4 | Construction of a ceRNA network

The miRNA target gene prediction algorithm miRanda (http://www.microrna.org/), Targetscan (http://www.targetscan.org/) and miRWalk (http://129.206.7.150/) were used for miRNA-mRNA target gene prediction.[23] miRanda and PITA (https://genie.weizmann.ac.il/pubs/mir07/mir07_exe.html) were used for target gene prediction of miRNA-lncRNA. Based on the predicted miRNA targeting relationship and expression relationship, miRNA-mRNA and miRNA-lncRNA relationship pairs with negative correlation were screened to construct an endogenous competitive ceRNA (lncRNA-miRNA-mRNA-Network) regulatory network.

2.5 | PPI protein regulatory network analysis

The Retrieval of Interacting Genes (STRING) database tool (string-db.org) was used to elucidate the interactive relationships

of DEmRNAs. The interacting pairs with confidence scores >0.4 were considered significant and retained. Based on the STRING results, the PPI network was visualized using Cytoscape software.[24]

2.6 | Cell culture and transfection

GC cell lines (AGS, MKN45, NCI-N87 and MGC803) and the human gastric epithelial cell line (GES-1) were purchased from the American Type Culture Collection (ATCC). All cell lines were cultured in Dulbecco's modified Eagle's medium (Gibco) supplemented with 10% (v/v) fetal bovine serum (Invitrogen) in a 5% CO_2 in air atmosphere at 37°C. pCDH-EF1a-RP11-1094M14.8 and si-RP11-1094M14.8 vectors were synthesized using siRNA (Shanghai, China) and transfected into GC cells using Lipofectamine 3000 (Invitrogen). Sequences of siRNA are shown in Table S3.

2.7 | Western blotting

Cells were harvested in RIPA Lysis Buffer, and were lysed by ultrasound treatment (#DH92-IIN; LAWSON). Supernatants were collected and protein concentrations were determined using Coomassie brilliant blue G250 stain (#C8420, Solarbio). Proteins were separated by SDS-PAGE and transferred to a Nylon membrane. Membranes were blocked in 5% Milk/TBS-T for 2 h at room temperature and incubated overnight at 4°C with primary antibodies and subsequently with HRP-conjugated secondary antibody. Antibodies against CXCL9 (#MAB392) and β-actin (#MAB8929) were purchased from B&D.

2.8 | Clinical subjects

In total, 60 patients with gastric cancer were recruited after the screening process, following approval by the Ethics Committee Board of the Fifth Affiliated Hospital of Zhengzhou University, Zhengzhou, China., Thirty tumor samples were collected from these patients during surgery at the Fifth Affiliated Hospital of Zhengzhou University.

2.9 | Immunohistochemistry analysis

The tissue specimens of GC patients were harvested, fixed in 10% buffered formalin, dehydrated, mounted in paraffin, and sectioned. Immunohistochemical staining was performed with antibodies against human CXCL9 (#ab9720, Abcam) and CD8α (#85336, CST). Two pathologists assessed all photographs. The German semiquantitative scoring system was used to assess the stain intensity and area extent. Each specimen received a score based on the intensity of stained cells (blank = 0, light yellow = 1, yellow = 2, and brown = 3) and the extent of stained cells (0% = 0, 1%-24% = 1, 25%-49% = 2, 50%-74% = 3, and 75%-100% = 4), and the immunoreactive score was calculated by multiplying the intensity score by the extent of stained cells.

2.10 | Quantitative real-time PCR (qRT-PCR)

Total RNA was extracted from GC cells and gastric tissues using TRIzol reagent (Thermo Fisher Scientific). A reverse transcription kit (TaKaRa Biotechnology) was used for reverse transcription. The StepOnePlus™ Real-Time PCR System (Thermo Fisher Scientific) was used to perform the qRT-PCR assay. GAPDH was used as the endogenous control to normalize lncRNA and mRNA expression, and Small RNA RNU6 (U6) was used for normalization of miRNA.[25] The relative expression level of the target RNA was calculated using $2^{-\Delta\Delta Ct}$. The primers used for amplification of targets are shown in Table S2.

2.11 | Survival analysis

The Univariate Cox regression model was used to analyze the relationship between overall survival and mRNA expression in GC patients, and a P-value < .05 was considered significant. The expression levels of the samples were grouped as high or low based on the cut-off point.[26]

3 | RESULTS

3.1 | Differentially expressed RNAs (DERNAs) in gastric cancer with different degrees of immune cell infiltration

We searched for gene expression microarrays of GC in the TCGA database, and the raw data were standardized for subsequent analysis.[27] Patients were defined as high expression or low expression based on the median expression levels of CD3, CD8, IFN-γ, and GZMB. We analyzed differentially expressed genes between the hot tumor group (111 patients with $CD3^+CD8^+IFN\text{-}\gamma^+GZMB^+$) and the cold tumor group (116 patients with $CD3^-CD8^-IFN\text{-}\gamma^-GZMB^-$).[28] The difference screening parameters were set as $P < .05$ and FDR < 0.05 and FC > 1.5. Differentially expressed RNAs, 97 lncRNAs, 46 miRNAs, and 1082 mRNAs, were identified (Figure 1A-C). Compared with the cold tumor group, 79 (80%) lncRNAs, 28 (60%) miRNAs, and 751 (69%) mRNAs were upregulated, and 18 (20%) lncRNAs, 19 (40%) miRNAs and 331 (31%) mRNAs were downregulated in the hot tumor group. The distributions of DERNAs were demonstrated using heatmaps and volcano plots. We analyzed the clinical characteristics of 2 groups from the TCGA data. The results are given

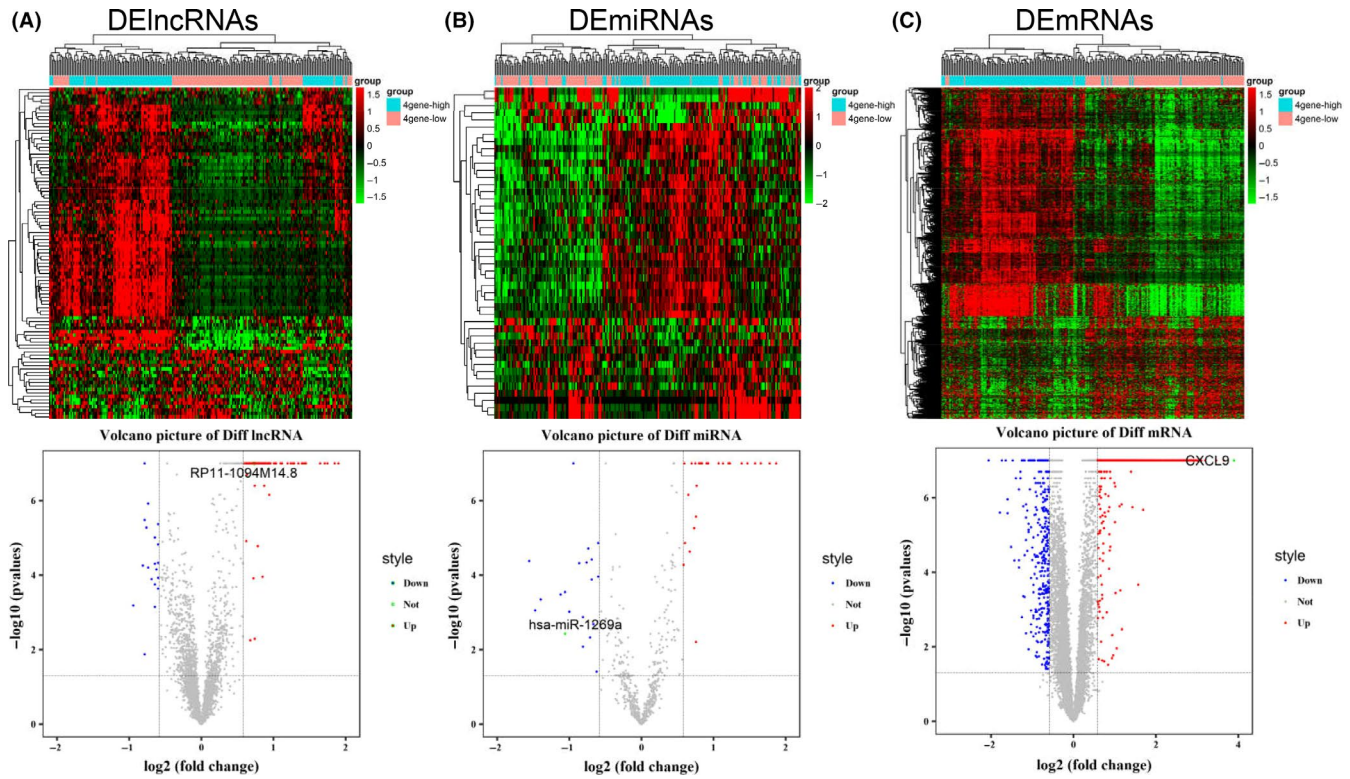

FIGURE 1 Identification of differentially expressed RNAs. Volcano plot and hot map of differentially expressed (A) lncRNAs (left), (B) miRNAs (middle), and (C) mRNAs (right). Red and green spots represent significant upregulated and downregulated RNAs, respectively

in Table S1. There was no difference in sex, age, and TNM stage. But, interestingly, there was a significant difference in histologic differentiation between the 2 groups and the histologic differentiation of patients was poor in the hot group compared with in the cold group. We considered that there might be suppression effects of other factors in this sub-group, like dietary habits, living environment, and so on.

3.2 | Functional enrichment analysis of the significant DERNAs

To investigate the potential functional implications of the 1082 DEmRNAs, we performed functional annotations of GO and KEGG of these DEmRNAs.[29] The enriched GO functions of significantly upregulated DEmRNAs were primarily involved in the IR, such as "T-cell receptor signaling pathway," "B cell receptor signaling pathway," and "positive regulation of B cell activation" (Figure 2A). Pathway analysis showed that the significantly upregulated DEmRNAs were significantly enriched in 25 KEGG pathways, such as "chemokine signaling pathway," "cytokine-cytokine receptor interaction," and "*Staphylococcus aureus* infection" (Figure 2C). These results suggested that the significantly upregulated DEmRNAs may influence the effects of immunotherapy for GC patients. The enriched GO functions for significantly downregulated DEmRNAs included cornification, cell differentiation, cell adhesion, and cell migration (Figure 2B). Some enriched KEGG pathways were also observed, and metabolic pathways were the most highly enriched pathways (Figure 2D).

3.3 | Construction of ceRNA network and Protein-Protein Interaction (PPI) network in gastric cancer with different degrees of immune cell infiltration

To identify whether these differentially expressed DERNAs existed in the competing endogenous regulating network, target genes of miRNA-mRNA and miRNA-lncRNA were predicted using the method of miRNA target basis factor predetermination, and a lncRNA-miRNA-mRNA ceRNA network of gastric cancer with different degrees of immune cell infiltration was constructed.[30] This network included 36 lncRNAs, 24 miRNAs, and 104 mRNAs. The expression levels of several immune-related genes, such as *CXCL9*, *CXCL10*, *CXCL13*, and *GZMB*, were upregulated in this ceRNA network. *CXCL9* was the most prominent gene, and was regulated by lncRNA RP11-1094M14.8 and miR-1269a (Figure 3A). Based on the ceRNA network, mRNA interaction relationships were identified using the STRING database with scores of >0.4, and 60 mRNAs were selected to construct the PPI network.[31] CXCL9 also showed important regulatory effects in the PPI network (Figure 3B). Given the differential expression of CXCL9 and the regulatory role of CXCL9 in the ceRNA network and PPI network,

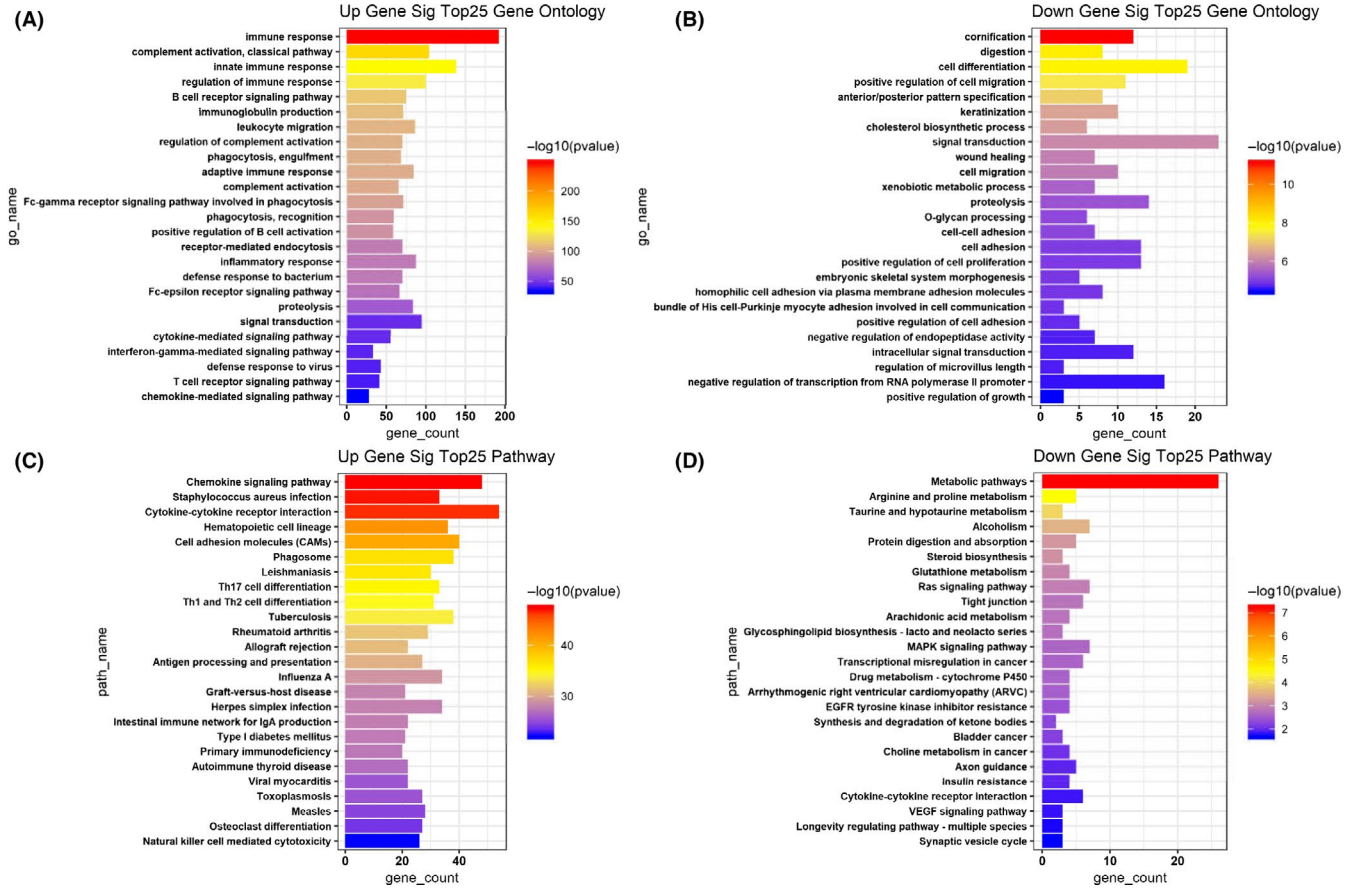

FIGURE 2 Gene Ontology (GO) and KEGG pathway enrichment analyses for the significant differentially expressed genes. A, The top 25 enriched GO biological processes of the significantly upregulated genes. B, The top 25 enriched GO biological processes of the significantly downregulated genes. C, The top 25 enriched KEGG pathways of the significantly upregulated genes. D, The top 25 enriched KEGG pathways of the significantly downregulated genes

CXCL9 may play an important role in the immunotherapy response for gastric cancer.[32]

3.4 | Correlation between CXCL9 and immune-related genes

Given the complexity of the immune system, the infiltration differences of immune cells in tumor tissues were analyzed between the 2 groups of GC patients. The results showed a significantly different infiltration pattern of immune cells between the hot tumor and cold tumor groups. $CD8^+$ T cells and activated $CD4^+$ T cells are positive regulatory immune cells that showed high infiltration in the hot tumors. Macrophage infiltration in the cold tumors was relatively high and the M1 subtype, which exerts tumor suppressive functions, was more likely to be found in the hot tumors. Notably, the infiltration of mast cells, which possess antigen-presenting functions in hot tumors, was significantly reduced; this finding suggests that other mechanisms of immune cell infiltration existed in these cells (Figure 4A). Pearson correlation coefficient (*r* value) was used for heatmap construction, and this heatmap was used to color these correlations. Correlation analysis showed that CXCL9 was significantly related to various immune cell-related genes; CXCL9 had the most obvious positive correlation with CD8 T cells and their functional factor GZMB. The preproprotein encoded by GZMB is secreted by natural killer (NK) cells and CTLs, and it generates an active protease that finally induces target cell apoptosis (Figure 4B). Correlation analysis between CXCL9 and immune infiltration was also performed using TIMER2.0 software (http://timer.cistrome.org/). CXCL9 was also found to be significantly and positively correlated with a variety of immune cells, such as $CD8^+$ T cells, $CD4^+$ T cells, NK cells, B cells, and so on. At the same time, immunosuppressive cells (myeloid-derived suppressor cells [MDSC], Macrophage M2) were significantly negatively correlated with CXCL9 (Figure S1). Consistent with our findings, CXCL9 played an important regulatory role in immune infiltration and was a key control point for regulation of "cold" gastric tumors into more immunologically activated "hot" tissues.

3.5 | Identification of a potential regulatory axis

A potential regulatory axis of RP11-1094M14.8/miR-1269a/CXCL9 was identified from the ceRNA network (Figure 5A). RP11-1094M14.8 and CXCL9 were significantly upregulated, and

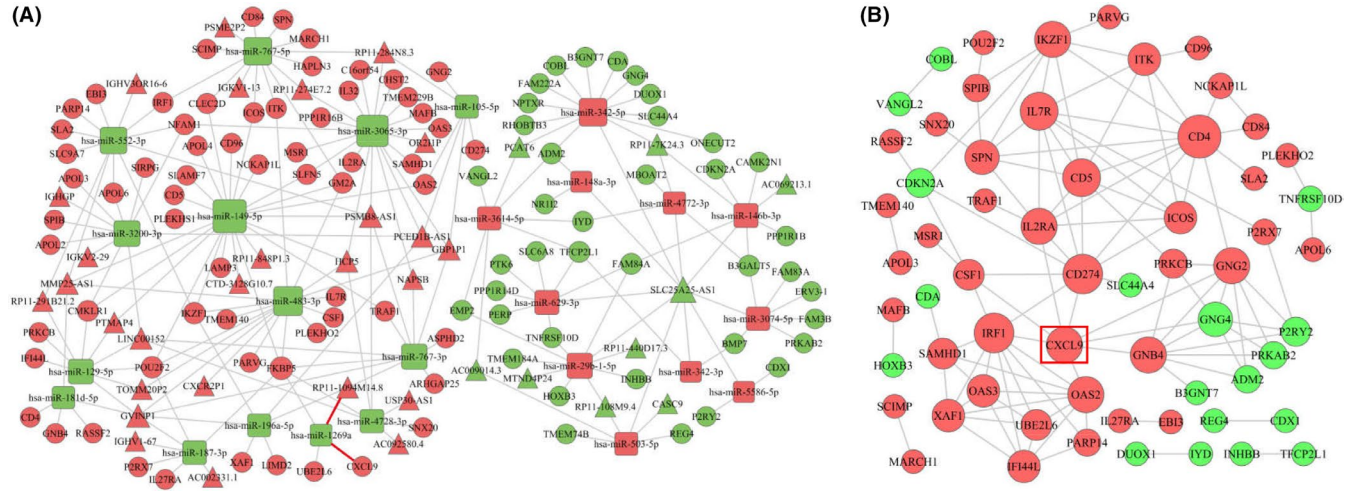

FIGURE 3 A, The ceRNA network in different degrees of immune infiltration in gastric cancer. Red nodes represent upregulation, and the green nodes represent downregulation. lncRNAs, miRNAs, and mRNAs are represented as triangles, squares, and circles, respectively. Gray edges indicate interactions between RNAs. B, The PPI network of DEmRNAs involved in the ceRNA network. Red nodes represent upregulation, and the green nodes represent downregulation. The size of the dots represents the regulatory capacity of the mRNA, and the larger dots, the stronger the regulatory capacity

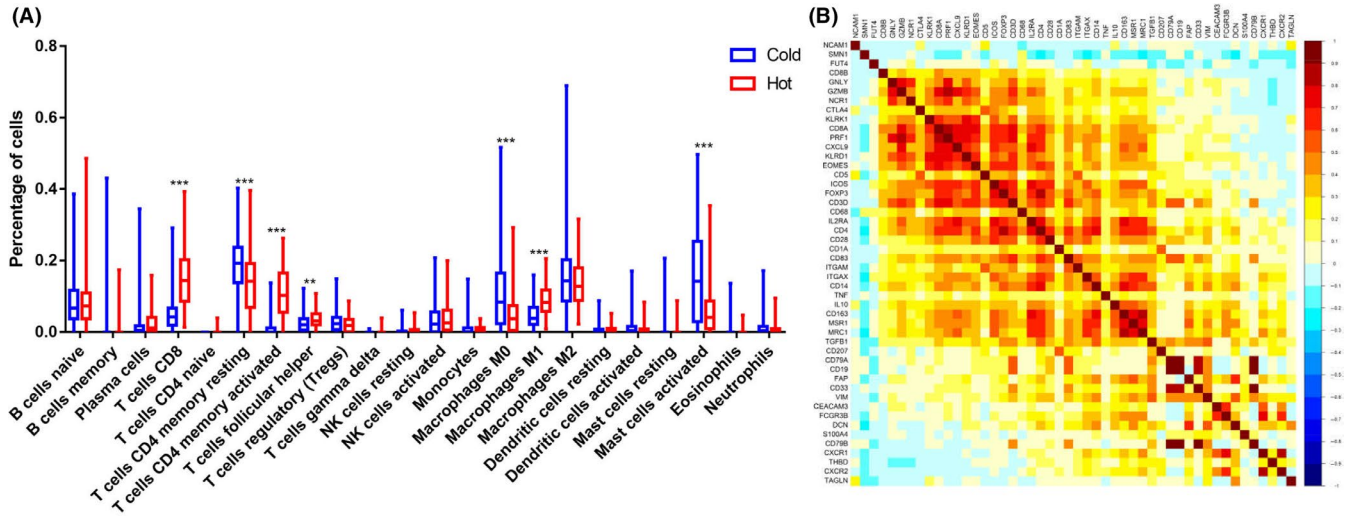

FIGURE 4 A, The differences in immune infiltration between the 2 groups (***$P < .0001$, **$P < .001$). B, Correlation analysis between CXCL9 and immune infiltration

miR-1269a was significantly downregulated in hot tumor tissue compared with cold tumor tissue (Figure S2A-C). Correlations of these 3 genes were analyzed. As expected, there was a significant correlation between PR11-1094M14.8 and CXCL9. However, there was no significant negative correlation between mir-1269a and PR11-1094M14.8, as well as CXCL9 (Figure S2D). This did not affect the present results, because the existing data analysis was based on targeted binding of these 3 genes instead of correlation analysis. Furthermore, qRT-PCR was performed to detected the expression levels of RP11-1094M14.8 , miR-1269a and CXCL9 in four GC cell lines, AGS, MKN45, NCI-N87, and MGC803, and the human gastric epithelial cell line GES-1(Table S2). The results showed that RP11-1094M14.8 and CXCL9 were underexpressed compared with expression in a normal gastric cell line, and miR-1269a was highly expressed in GC cell lines (Figure 5B-D). To further determine the expression of CXCL9, protein expression was detected by western blot (Figure S3). These findings were consistent with our expectation that CXCL9 had low expression in GC cell lines. NCI-N87 cells exhibited a higher expression level in RP11-1094M14.8 compared with other GC cell lines, in contrast with the MKN45 cells, which showed a lower expression level. Therefore, NCI-N87 cells were selected for RP11-1094M14.8 knockdown using siRNA (Table S3), and MKN45 cells were chosen for overexpression (Figure 5E,F). We detected the expression levels of *CXCL9* in different treatment groups using qRT-PCR. The results showed that gene expression of *CXCL9* was upregulated when *RP11-1094M14.8* was overexpressed, and gene expression of *CXCL9* was downregulated when *RP11-1094M14.8* was knocked down (Figure 5G). In contrast, miR-1269a expression

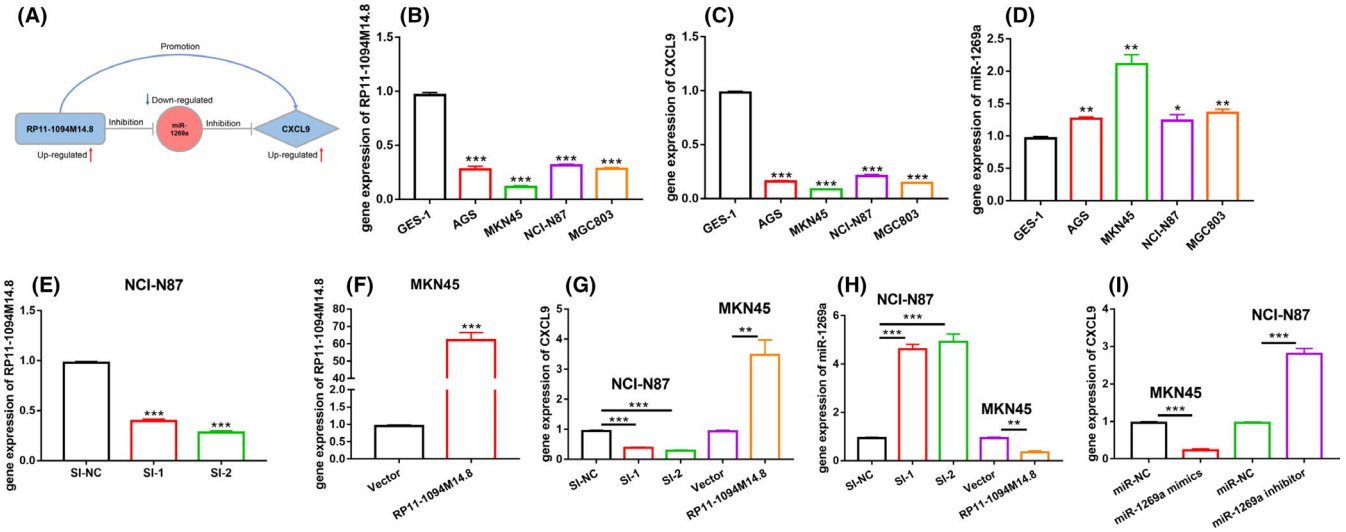

FIGURE 5 Experimental validation of the RP11-1094M14.8/miR-1269a/CXCL9 axis. A, A potential regulatory axis of RP11-1094M14.8/miR-1269a/CXCL9, which perfectly conformed to the ceRNA theory. B, RP11-1094M14.8 was downregulated in GC cell lines (AGS, NCI-N87, MKN-45, MGC803) compared with gastric epithelial GES-1 cells. C, CXCL9 was downregulated in GC cell lines compared with gastric epithelial GES-1 cells. D, miR-1269a was upregulated in GC cell lines compared with gastric epithelial GES-1 cells. E, RP11-1094M14.8 was knocked down in MKN-45 cells, and the effects of knockdown were measured using qRT-PCR. F, RP11-1094M14.8 was overexpressed in MKN-45 cells, and the effects of overexpression was measured using qRT-PCR. G, H, The expression levels of miR-1269a and CXCL9 after knockdown or overexpression of RP11-1094M14.8 in NCI-N87 or MKN-45 cells. I, The expression levels of CXCL9 after knockdown or overexpression of miR-1269a in NCI-N87 or MKN-45 cells. Data represent 1 of the 3 independent experiments with similar results (***$P < .0001$, **$P < .001$)

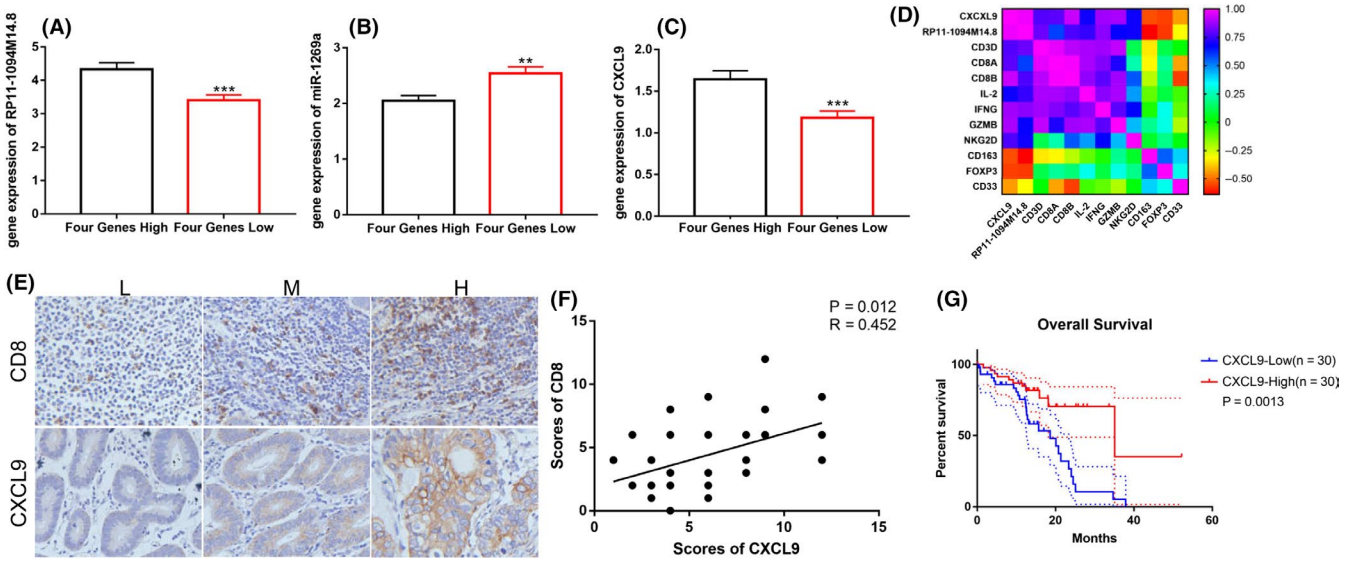

FIGURE 6 Clinical specimens verified the control axis and immune infiltration. Based on the expression values of CD3, CD8, IFN-γ, and GZMB, Clinical samples we screened were defined as hot and cold tumor. Hot group exhibited high expression of the 4 genes (Four Genes High). Cold group exhibited low expression of the 4 genes (Four Genes Low). A, RP11-1094M14.8 was highly expressed in high immune infiltration GC. B, miR-1269a exhibited low expression in high immune infiltration GC. C, CXCL9 was highly expressed in high immune infiltration GC (***$P < .0001$, **$P < .001$). D, Immuno-correlation analysis of CXCL9 and RP11-1094M14.8. Based on the expression values of CXCL9, the clinical specimens were divided into 2 groups. E, F, Immunohistochemical analysis was performed to evaluate the correlation between CD8 and CXCL9 protein expression. G, Kaplan–Meier curve of CXCL9 that significantly correlated with overall survival

significantly increased after *RP11-1094M14.8* knockdown in NCI-N87 cells and decreased after *RP11-1094M14.8* overexpression in MKN45 cells, as determined using qRT-PCR (Figure 5H). Then, we purchased mimics and an inhibitor of miR-1269a and detected changes in gene expression of *CXCL9* caused by changes in miR-1269a. In line with expectations, miR-1269a acted as a sponge of *CXCL9* expression, *CXCL9* levels were downregulated by miR-1269a mimics and upregulated by the miR-1269a inhibitor (Figure 5I).

3.6 | Immunity role of CXCL9 in clinical samples

To date, tumor immunotherapy has primarily focused on T-cell-mediated cytotoxicity. IFN-γ and GZMB as markers of T-cell function will likely be missing following T-cell depletion induced by the tumor microenvironment. Infiltration of exhausted T cells could have a subsequent negative fatigue effect on later immunotherapy, this type of tumor cannot be defined as a "hot" tumor. Conversely, to improve the validity of these analyses, more refined grouping is necessary. Therefore, eliminating such cases from samples collected was executed. Screened clinical samples were defined as hot or cold tumors. One group exhibited high expression of the 4 genes ($CD3^+CD8^+IFN\text{-}\gamma^+GZMB^+$) and was defined as hot tumors. The other group exhibited low expression of the 4 genes ($CD3^-CD8^-IFN\text{-}\gamma^-GZMB^-$) and was defined cold tumors. We detected the expression of *RP11-1094M14.8*, miR-1269a and *CXCL9* (Figure 6A-C). *RP11-1094M14.8* and *CXCL9* were highly expressed in hot tumors, and the expression of miR-1269a was low in hot tumors. The correlation between *CXCL9* and immune-related genes was investigated. A heatmap was constructed using the Pearson correlation coefficient (*r*) of these genes. This heatmap was used to color these correlations: pink indicated positive correlations, and the color intensity indicated the strength of correlation. The results showed that CXCL9 was distinctly positively correlated with cytotoxic cells but negatively correlated with immunosuppressive cells (Figure 6D). Therefore, we performed immunohistochemical analyses to determine and compare the expression levels of CD8 and CXCL9 from 30 GC tissues (Figure 6E,F). The proportion of $CD8^+$ T cells strongly correlated with CXCL9 levels in GC tissues, which indicated that $CD8^+$ T-cell recruitment in vivo was associated with secretion of CXCL9. The results of the pathological parameter analysis showed that low expression of CXCL9 correlated with advanced TNM stage ($P = .0106$) and lymphovascular invasion ($P = .013$) (Table S4). Low expression of CXCL9 correlated with a poor prognosis for GC patients (Figure 6G).

4 | DISCUSSION

Gastric cancer has a high mortality rate, and threatens human life and health.[33] The extremely poor prognosis of patients with gastric cancer greatly promotes the development of an effective treatment measure.[34] Compared with traditional treatment, immunotherapy is a new treatment that shows great potential in the treatment of tumors. However, some patients do not benefit from it.[35] Therefore, it is important to find indicators to predict whether patients will benefit from immunotherapy.[36] Key to improving outcomes from immunotherapy is the detailed understanding of the cellular and molecular mechanisms. Recent studies have shown that ncRNAs play important roles in cancer initiation, progression, and immune regulation. miRNAs and lncRNAs are important parts of ncRNAs, and have received more attention from medical researchers.[37] We expected to find new indicators to detect if patients would benefit from immunotherapy. Here, we specifically explored RP11-1094M14.8/miR-1269a/CXCL9 induced immune responses in patients with GC at the level of gene expression signatures and infiltrative immune cells.

The present study analyzed the information from gastric cancer patients present in TCGA database. The biological functions of DEmRNAs in 2 groups were investigated using KEGG pathway analysis and GO analysis. Results were consistent with existing reports and revealed that these DEmRNAs were significantly associated with changes in immune function and the chemokine signaling pathway. Most importantly, significant differences were found in the activation and function of T cells and NK cells, which was in line with our expectations. To find the key gene for immunity regulation, a ceRNA network and a PPI network were constructed using the DERNAs. *CXCL9* was the most significantly different gene in these networks, all results evidently pointed to CXCL9 as a gatekeeper in the immunity regulation. CXCL9 primarily mediates the infiltration of lymphocytes into lesions and inhibits tumor growth.[38-40] Gorbachev et al[41] showed with in vivo models that cancer cells deficient in CXCL9 were more likely to result in tumors than cells expressing CXCL9 and CXCL10. The facilitation of CXCL9 expression on monoclonal antibody therapy was reported. Our focus on CXCL9 as a key tumor cell-intrinsic regulator of immune phenotypes stemmed from mixing experiments that showed that low T-cell infiltration exerted a dominant effect. CXCL9 was also found to be significantly and positively correlated with a variety of immune cells such as NK cells, B cells and dendritic cells (DCs). Immunosuppressive cells (MDSC, Macrophage M2) were significantly negatively correlated with CXCL9. Consistent with our view, CXCL9, with an important regulatory role in immune infiltration, was a key control point for regulation of "cold" prostate tumors into more immunologically activated "hot" tissues. Our findings also indicated that tumor cell-derived CXCL9, which is a molecular "switch" of T-cell infiltration in the tumor microenvironment (TME) phenotype, had corresponding effects on the poor prognosis of patients.

Based on the results of the ceRNA network and PPI network, a potential RP11-1094M14.8/miR-1269a/CXCL9 regulatory axis was proposed. Expression levels and regulatory relationship were further demonstrated by cell experiment and clinical specimens. These findings suggested a new mechanism in CXCL9 secretion. This finding can provide a new diagnostic index for whether patients would benefit from immunotherapy. Further analysis showed that low expression levels of CXCL9 were associated with lymphovascular invasion and advanced TNM stage, and these patients showed poor prognosis. Immunoassay results showed that CXCL9 positively correlated with molecules associated with the activation and function of T cells and NK cells; immunosuppressive molecules showed the opposite correlation, which suggests the role of CXCL9 in immune regulation. This further confirmed our initial results. In future research, we will use a chimeric antigen receptor (CAR) T-cell therapeutic model to study CXCL9.

In conclusion, we provided a comprehensive view of the underlying mechanism for the progression of different degrees of immune infiltration of gastric cancer by constructing a ceRNA regulatory network and axis. We proposed an axis in which

RP11-1094M14.8 'sponges up' miR-1269a to regulate CXCL9 expression. These findings were validated in clinical samples and cell lines using qRT-PCR. We suggest that this regulatory axis exerts a critical role in the immune cell infiltration of GC. CXCL9 may be used as a potential diagnostic indicator for predicting the benefit of immunotherapy in GC patients. There are some limitations to our study, further tests are needed for validation. No further in vivo experiments were used to validate these results, and the exact mechanisms of immune infiltration induced by CXCL9 must be further investigated.

ETHICAL APPROVAL AND CONSENT TO PARTICIPATE

The research protocol was reviewed and approved by the Ethics Committee of Zhengzhou University, and informed consent was obtained from all participants included in the study, in agreement with institutional guidelines.

ACKNOWLEDGMENTS

We thank the patients and their families for their signed informed consent forms for clinical sample experiments. This work was supported by grants from the Zhengzhou Major Collaborative Innovation Project (No. 18XTZX12003); Excellent Foreign Scientist Studio of Henan Province in China (grant number GZS2018001); Medical Service Capacity Improvement project of Henan Province in China (grant number Yu Wei Medicine [2017] No. 66); Medical Science and Technology Project of Henan Province in China (grant number 2018020224); and the National Natural Science Foundation of China (grant number 31471330).

AUTHOR CONTRIBUTION

KZ, LZ, YM designed this work and analyzed the data; YCT, FFR, helped or performed experiments and analyses; BL helped for providing tumor samples; LZ, YM helped in revision of the manuscript; KZ, YZ and PYZ wrote the manuscript.

DISCLOSURES

The authors declare that they have no competing interests.

CONSENT FOR PUBLICATION

Not applicable.

DATA AVAILABILITY STATEMENT

The datasets used and/or analyzed during the current study are available from the corresponding author on reasonable request.

ORCID

Yi Zhang https://orcid.org/0000-0001-9861-4681
PengYuan Zheng https://orcid.org/0000-0003-1647-0253

REFERENCES

1. Van Cutsem E, Sagaert X, Topal B, Haustermans K, Prenen H. Gastric cancer. *Lancet*. 2016;388:2654-2664.
2. Tang W, Pan X, Han D, et al. Clinical significance of CD8+ T cell immunoreceptor with Ig and ITIM domains+ in locally advanced gastric cancer treated with SOX regimen after D2 gastrectomy. *OncoImmunology*. 2019;8:e1593807.
3. Choi IJ, Kook MC, Kim YI, et al. *Helicobacter pylori* therapy for the prevention of metachronous gastric cancer. *N Engl J Med*. 2018;378:1085-1095.
4. Campos-Carrillo A, Weitzel JN, Sahoo P, et al. Circulating tumor DNA as an early cancer detection tool. *Pharmacol Ther*. 2020;207:107458.
5. Wen TI, Wang Z, Li YI, et al. A four-factor immunoscore system that predicts clinical outcome for stage II/III gastric cancer. *Cancer Immunol Res*. 2017;5:524-534.
6. Sukocheva OA, Furuya H, Ng ML, et al. Sphingosine kinase and sphingosine-1-phosphate receptor signaling pathway in inflammatory gastrointestinal disease and cancers: a novel therapeutic target. *Pharmacol Ther*. 2020;207:107464.
7. Brown EM, Kenny DJ, Xavier RJ. Gut microbiota regulation of T cells during inflammation and autoimmunity. *Annu Rev Immunol*. 2019;37:599-624.
8. Miao L, Qi J, Zhao QI, et al. Targeting the STING pathway in tumor-associated macrophages regulates innate immune sensing of gastric cancer cells. *Theranostics*. 2020;10:498-515.
9. Daniel SK, Seo YD, Pillarisetty VG. The CXCL12-CXCR4/CXCR7 axis as a mechanism of immune resistance in gastrointestinal malignancies. *Semin Cancer Biol*. 2020;65:176-188.
10. Xu Z-J, Gu Y, Wang C-Z, et al. The M2 macrophage marker: a novel prognostic indicator for acute myeloid leukemia. *Oncoimmunology*. 2020;9:1683347.
11. Urdinez J, Boro A, Mazumdar A, et al. The miR-143/145 cluster, a novel diagnostic biomarker in chondrosarcoma, acts as a tumor suppressor and directly inhibits Fascin-1. *J Bone Miner Res*. 2020;35:1077-1091.
12. Akin Telli T, Bregni G, Camera S, Deleporte A, Hendlisz A, Sclafani F. PD-1 and PD-L1 inhibitors in oesophago-gastric cancers. *Cancer Lett*. 2020;469:142-150.
13. Leclerc M, Mezquita L, Guillebot De Nerville G, et al. Recent advances in lung cancer immunotherapy: input of T-cell epitopes associated with impaired peptide processing. *Front Immunol*. 2019;10:1505.
14. Wang C-J, Zhu C-C, Xu J, et al. Correction to: The lncRNA UCA1 promotes proliferation, migration, immune escape and inhibits apoptosis in gastric cancer by sponging anti-tumor miRNAs. *Mol Cancer*. 2019;18:129.
15. Yang X-Z, Cheng T-T, He Q-J, et al. LINC01133 as ceRNA inhibits gastric cancer progression by sponging miR-106a-3p to regulate APC expression and the Wnt/β-catenin pathway. *Mol Cancer*. 2018;17:126.
16. Huang J, Chen Y-X, Zhang B. IGF2-AS affects the prognosis and metastasis of gastric adenocarcinoma via acting as a ceRNA of miR-503 to regulate SHOX2. *Gastric Cancer*. 2020;23:23-38.
17. Zhang G, Li S, Lu J, et al. LncRNA MT1JP functions as a ceRNA in regulating FBXW7 through competitively binding to miR-92a-3p in gastric cancer. *Mol Cancer*. 2018;17:87.
18. Han Y, Wu N, Jiang M, et al. Long non-coding RNA MYOSLID functions as a competing endogenous RNA to regulate MCL-1 expression by sponging miR-29c-3p in gastric cancer. *Cell Prolif*. 2019;52:e12678.
19. Song Y-X, Sun J-X, Zhao J-H, et al. Non-coding RNAs participate in the regulatory network of CLDN4 via ceRNA mediated miRNA evasion. *Nat Commun*. 2017;8:289.
20. Tay Y, Kats L, Salmena L, et al. Coding-independent regulation of the tumor suppressor PTEN by competing endogenous mRNAs. *Cell*. 2011;147:344-357.

21. Li J, Byrne KT, Yan F, et al. Tumor cell-intrinsic factors underlie heterogeneity of immune cell infiltration and response to immunotherapy. *Immunity*. 2018;49:178-193 e177.
22. Zhang T, Jiang M, Chen L, Niu B, Cai Y. Prediction of gene phenotypes based on GO and KEGG pathway enrichment scores. *Biomed Res Int*. 2013;2013:870795.
23. Lv J, Fan H-X, Zhao X-P, et al. Corrigendum to "Long non-coding RNA unigene 56159 promotes epithelial-mesenchymal transition by acting as a ceRNA of miR-140-5p in hepatocellular carcinoma cells" [Canc. Lett. 382 (2016) 166–175]. *Cancer Lett*. 2019;472:181-182.
24. Chu A, Liu J, Yuan Y, Gong Y. Comprehensive analysis of aberrantly expressed ceRNA network in gastric cancer with and without *H pylori* infection. *J Cancer*. 2019;10:853-863.
25. Pan H, Guo C, Pan J, et al. Construction of a competitive endogenous RNA network and identification of potential regulatory axis in gastric cancer. *Front Oncol*. 2019;9:912.
26. Li G, Han L, Ren F, Zhang R, Qin G. Prognostic value of the tumor-specific ceRNA network in epithelial ovarian cancer. *J Cell Physiol*. 2019;234:22071-22081.
27. Russi S, Calice G, Ruggieri V, et al. Gastric normal adjacent mucosa versus healthy and cancer tissues: distinctive transcriptomic profiles and biological features. *Cancers (Basel)*. 2019;11:1248.
28. Newman JH, Chesson CB, Herzog NL, et al. Intratumoral injection of the seasonal flu shot converts immunologically cold tumors to hot and serves as an immunotherapy for cancer. *Proc Natl Acad Sci USA*. 2019;117:1119-1128.
29. Yuan F, Lu L, Zhang Y, Wang S, Cai Y-D. Data mining of the cancer-related lncRNAs GO terms and KEGG pathways by using mRMR method. *Math Biosci*. 2018;304:1-8.
30. Naorem LD, Prakash VS, Muthaiyan M, Venkatesan A. Comprehensive analysis of dysregulated lncRNAs and their competing endogenous RNA network in triple-negative breast cancer. *Int J Biol Macromol*. 2019;145:429-436.
31. Lv Y, He XY, Li D, Liu T, Wen GQ, Li J. Sex-specific and opposite modulatory aspects revealed by PPI network and pathway analysis of ischemic stroke in humans. *PLoS One*. 2020;15:e0227481.
32. de la Iglesia JV, Slebos RJC, Martin-Gomez L, et al. Effects of tobacco smoking on the tumor immune microenvironment in head and neck squamous cell carcinoma. *Clin Cancer Res*. 2019;26:1474-1485.
33. Zhang H, Schaefer A, Wang Y, et al. Gain-of-function RHOA mutations promote focal adhesion kinase activation and dependency in diffuse gastric cancer. *Cancer Discov*. 2019;10:288-305.
34. Slomski A *H. pylori* treatment may reduce long-term gastric cancer risk. *JAMA*. 2019;322:1948.
35. Sidaway P. Immunotherapy-responsive gastric cancers identified. *Nat Rev Clin Oncol*. 2018;15:582.
36. Ding N, Zou Z, Sha H, et al. iRGD synergizes with PD-1 knockout immunotherapy by enhancing lymphocyte infiltration in gastric cancer. *Nat Commun*. 2019;10:1336.
37. Liu Z, Pan HM, Xin L, et al. Circ-ZNF609 promotes carcinogenesis of gastric cancer cells by inhibiting miRNA-145-5p expression. *Eur Rev Med Pharmacol Sci*. 2019;23:9411-9417.
38. Tokunaga R, Zhang WU, Naseem M, et al. CXCL9, CXCL10, CXCL11/CXCR3 axis for immune activation – a target for novel cancer therapy. *Cancer Treat Rev*. 2018;63:40-47.
39. Ohtani H, Jin Z, Takegawa S, Nakayama T, Yoshie O. Abundant expression of CXCL9 (MIG) by stromal cells that include dendritic cells and accumulation of CXCR3+ T cells in lymphocyte-rich gastric carcinoma. *J Pathol*. 2009;217:21-31.
40. Dangaj D, Bruand M, Grimm AJ, et al. Cooperation between constitutive and inducible chemokines enables T cell engraftment and immune attack in solid tumors. *Cancer Cell*. 2019;35:885-900.e810.
41. Gorbachev AV, Kobayashi H, Kudo D, et al. CXC chemokine ligand 9/monokine induced by IFN-gamma production by tumor cells is critical for T cell-mediated suppression of cutaneous tumors. *J Immunol*. 1950;2007(178):2278-2286.

SUPPORTING INFORMATION

Additional supporting information may be found online in the Supporting Information section.

How to cite this article: Zhang K, Zhang L, Mi Y, et al. A ceRNA network and a potential regulatory axis in gastric cancer with different degrees of immune cell infiltration. *Cancer Sci*. 2020;111:4041–4050. https://doi.org/10.1111/cas.14634